

# Immune profiling in human breast cancer using high-sensitivity detection and analysis techniques

Brendon J Coventry<sup>1</sup>, Michael J Weightman<sup>1</sup>, John Bradley<sup>2</sup> and John M Skinner<sup>3</sup>

<sup>1</sup>Discipline of Surgery, University of Adelaide, Royal Adelaide Hospital, Adelaide, South Australia 5000, Australia

<sup>2</sup>Department of Clinical Immunology, Flinders University, Adelaide, South Australia 5001, Australia

<sup>3</sup>Department of Pathology, Flinders University, Adelaide, South Australia 5001, Australia

**Corresponding author:** Brendon J Coventry. Email: [brendon.coventry@adelaide.edu.au](mailto:brendon.coventry@adelaide.edu.au)

## Summary

**Objectives:** Evaluation of immune profiles in human breast cancer using high-sensitivity detection and analysis methods.

**Design:** Cohort comparative analysis studies of breast tissue.

**Setting:** Human hospital and laboratory healthcare facilities.

**Participants:** Women over 18 years.

**Main outcome measures:** Evaluation of the comparative immunophenotype of human breast carcinoma and normal breast tissues.

**Results:** Leukocyte density and specific subgroups of lymphocytes and macrophages were generally higher in breast cancers compared to normal breast tissues. CD3, CD4, CD45RO, CD45RA(2H4), CD45 and HLA Class II (on TIL) were significantly expressed on breast tumour tissues compared with normal tissues ( $p < .01$ ). Some 30% of T-cells were  $\gamma\delta$ -TCR positive, but the majority were  $\alpha\beta$ -TCR in type. CD19 (B-cell), CD14 (FMC32 and 33) and HLA Class I levels (epithelial and TIL) showed no significant differences. IL-2 $\alpha$  receptor expression was low or absent on most TIL.

**Conclusions:** High-sensitivity and image analysis techniques permitted accurate characterisation of the TIL infiltrate for immune profiling. Breast carcinoma showed predominance of CD4 T-cells of mainly memory phenotype. Normal breast tissues showed low leukocyte infiltration. Further correlation of these findings with clinical outcome, including survival, is proceeding with encouraging results.

## Keywords

breast cancer, tumour-infiltrating leukocytes/lymphocytes, TIL, high sensitivity immunostaining, video image analysis, VIA, cellular quantitation, CD3, CD4, CD8, CD45, CD56, CD16, CD25, HLA

improved survival following surgical resection of the tumour,<sup>5–9</sup> has been additionally associated with improved response to adjuvant and neo-adjuvant chemo-radiotherapy,<sup>10–13</sup> and has also recently associated with PD-1/PDL-1 expression.<sup>14</sup>

The specific lymphocytic phenotype has been less clearly defined. Both CD8<sup>+</sup> cytotoxic T-cells and CD4<sup>+</sup> helper T-cells are widely considered to protect against oncogenesis,<sup>15–17</sup> while recent data indicate that CD4<sup>+</sup>CD25<sup>+</sup> regulatory T-cells may actually suppress the antitumoral immunological response.<sup>18</sup> Other authors have found that increased expression of CD3<sup>+</sup> has been associated with improved treatment response.<sup>19,20</sup> The precise qualitative details of the nature of the infiltrate have been complex to understand, and some disparity remains within the literature regarding the major subpopulations within the lymphoid infiltrate in normal breast and breast carcinoma tissues, particularly regarding the predominance of CD4<sup>+</sup> or CD8<sup>+</sup> cells.<sup>15,16,21</sup>

The underlying causes of the variability regarding the characterisation of TILs may partly reside in the sensitivity of the detection methods used. Most studies have used lower sensitivity, non-heavy metal enhanced methods to identify the component cell types of the infiltrate. Consequently, cells with surface molecules in low copy number may not be demonstrated by standard diaminobenzidine immunoperoxidase staining. However, at least a seven-fold greater detection sensitivity for low copy number surface molecules can be achieved using heavy metal enhanced DAB methods to reveal greater numbers of positive cells than unenhanced DAB staining.<sup>22,23</sup>

Another perhaps even more crucial reason for the considerable variation in the findings of past studies resides in techniques used for quantitation of cellular immunophenotypes. Traditionally, manually graded microscopic quantitation methods have been used almost universally to measure and compare results. Slides of tissue sections are assigned a representative grade of density on a discontinuous ordinal scale such

## Introduction

Leukocytes are consistently associated with human breast carcinomas. T-cells represent the predominant cell type within infiltrating leukocyte/lymphocyte (TIL) populations.<sup>1–4</sup> An increased density of TILs in breast cancer appears broadly associated with

as 0, +/-, +, ++, +++ and +++++. Considerable intra- and interobserver errors exist within standard light microscopic direct manual quantitation methods.<sup>24–26</sup> Video image analysis systems have provided a more standardised and objective method of cell quantitation, although manual quantitation still remains the standard methodology used. Comparison of mononuclear infiltrates from different tumours is however an onerous and imprecise task using direct visual methods.<sup>27</sup> Therefore, the novel technique of computer-assisted video image analysis, previously reported by Coventry et al.,<sup>28</sup> offers an approach towards quantitation of cellular infiltrate within breast cancer with better standardisation and reproducibility.

If the immunophenotype could be accurately determined in breast cancers, then the association with longer term survival could potentially be more reliably evaluated.

The aim of the present study was to use monoclonal antibody immunostaining with higher sensitivity nickel-enhanced DAB immunochemistry and compare both standard manual visual quantitation and video image analysis quantitation methods to define the immune profile (major TIL subpopulations) of normal breast and breast carcinoma tissues, including the relative balance of CD4<sup>+</sup> or CD8<sup>+</sup> cells.

## Methods

The immunostaining and analysis methodology for this study was described previously in Coventry et al.<sup>28</sup>

### Preparation and immunostaining of breast tissues

Comparison was made between 25 primary breast carcinoma and 10 histologically normal tissue samples taken directly following surgical resection, immediately cryopreserved and then sectioned according to protocol. The samples were taken from surgical specimens by the attending pathologist during surgical pathology dissection at Flinders Medical Centre and Flinders University, Adelaide. Investigators were not involved in the surgery or pathology reporting. Studies were approved by the Institutional Human Research Ethics Committee and data were deidentified for analysis and reporting. Samples were evaluated by investigators without knowledge of the pathology details to avoid bias. Normal breast samples were taken from breast reduction specimens and confirmed non-malignant breast tissues.

### Monoclonal antibodies

Multiple primary murine antihuman monoclonal antibodies (Table 1) were used for staining. All were

incubated in a humid chamber overnight for adequate binding and avoidance of drying. Each antibody was titrated on human tonsil and lymph node sections for optimum dilution before application on breast sections, to obtain high contrast from background. Negative isotypic control antibodies and relevant positive control tissues were included.

### Immunostaining

Horse antimouse biotinylated second antibody was incubated for 30 minutes, with endogenous peroxidase blocking using a 1% solution of H<sub>2</sub>O<sub>2</sub> in 70% ethanol. Avidin–biotin immunoperoxidase complex was incubated for 45 minutes using Vectastain kit reagents (Vector Laboratories, Burlingame, CA). Importantly, 3,3'-diaminobenzidine (Sigma, St Louis, MO) enhanced with 0.08% nickel chloride was used for higher sensitivity. Three five-minute phosphate-buffered saline washes between steps ensured adequate removal of non-bound antibodies and reagents.

### Direct microscopic visual quantitation

The stained tissue sections were scored on a grading system of 0, +/-, +, ++, +++ or +++++ by three independent observers (BJC, JB, JMS) to evaluate average density of cells per unit area of section at ×250 magnification. The results of the 25 breast carcinoma and 10 normal breast tissue samples were analysed for the degree of cellular infiltrate for each antibody. A grade was assigned for each tissue, both normal and tumour, and then recorded.

### Computer-assisted video image analysis quantitation

Twenty of the stained tissue sections were examined for quantitation using video image analysis, as previously described.<sup>28</sup> Briefly, a microscope head-mounted video camera captured serial images across an immunostained tissue section. Thresholds were chosen to detect reaction product, and total pixel density measurements were made after background correction.<sup>28</sup> Data sets for each consecutive video field were made, and graphs were plotted for each tissue section scanned using Statgraphics time-series analysis (version 4.0; Statpoint Technologies, Warrenton, VA).

### Statistics

Statistical analyses were performed using *SAS version 9.2* (SAS Institute Inc., Cary, NC) and *SPSS Statistics version 20* (IBM, Armonk, NY).

**Table 1.** Monoclonal antibodies used.

MoAb	Antigen	Subclass	Concentration	Source
Leu 4	CD3	IgG <sub>1</sub>	1/50	BD
DakoT4	CD4	IgG <sub>1</sub>	1/20	Dakopatts
Leu 2a	CD8	IgG <sub>1</sub>	1/50	BD
UCHL1	CD45R <sub>o</sub>	IgG <sub>2a</sub>	1/100	Beverley
FMC44	CD45Ra	IgG <sub>1</sub>	S/N	Zola
FMC51	CD45R	IgG <sub>1</sub>	1/05	Zola
$\alpha$ Tac	CD25	IgG <sub>1</sub>	1/25	BD
4F2	CD98	IgG <sub>2a</sub>	1/40	BD
2H4	CD45Ra	IgG <sub>1</sub>	1/100	Coulter
$\delta$ T	$\delta$ TCR	IgG <sub>1</sub>	1/400	Brenner
$\beta$ F <sub>1</sub>	$\beta$ TCR	IgG <sub>1</sub>	1/10	T-cell Sci
FMC14	HLA-D	IgG <sub>1</sub>	S/N	Zola
FMC63	CD19/21	IgG <sub>1</sub>	1/50	Zola
FMC32	CD14	IgG <sub>1</sub>	1/10	Zola
FMC33	CD14	IgG <sub>1</sub>	S/N	Zola
Leu 19	CD16	IgG <sub>1</sub>	1/10	BD
Leu 7	CD57	IgM	1/10	BD
Leu 22	CD43	IgG <sub>1</sub>	1/200	BD
Leu 23	CD69	IgG <sub>1</sub>	1/10	BD

## Results

### Descriptive statistics

The patient and tumour characteristics are detailed in Table 2. A total of 25 patients were included in the study, with a median age of 61 years (range 31–85). The histology from the vast majority of patients (20; 80%) were of the invasive ductal tumour type (not otherwise specified), with 5 (20%) demonstrating each of undifferentiated (1), invasive lobular (2), medullary (1) and mixed invasive ductal/lobular tumour (1). Eleven patients (44%) were reported as having poorly differentiated (high-grade) tumours, 11 being moderately differentiated (intermediate-grade), 2 as well differentiated (low-grade) and 1 not defined. The mean tumour size was 34.7 mm (range 14–190 mm). Fourteen patients (56%) of the cohort

were lymph node positive. Regarding TNM staging, 7 (28%) were classed as being TNM Stage I, with 12 (48%) being Stage II, 4 (16%) were Stage III and 2 were not available.

### Direct visual quantitation

The frequency percentage of visual grades assigned for the 25 breast carcinoma and 10 normal breast tissue samples tissues were represented on histograms (Figure 1) displaying each grade of cellular infiltrate for each specific monoclonal antibody.

**Normal breast tissues.** Low numbers of lymphocytes were present in within normal breast tissue. T-cells predominated with a T4:T8 ratio of 1 and an equal proportion of naive CD45RA to memory CD45RO cells. Most of the T-cells were  $\alpha\beta$ -TCR in type with

**Table 2.** Patient and primary breast tumour details.

Age	Lymph node status	Tumour type	Tumour size (mm)	TNM stage	Differentiation
85	+ (4/10)	ID	35	II	Mod.
61	+ (4/15)	ID	18	II	Well
53	– (0/15)	ID	25	II	Poor
79	+ (1/1)	ID	25	III	Poor
46	+ (2/7)	ID	15	II	Poor
53	+(19/20)	ID	30	II	Poor
53	– (0/11)	ID	15	I	Mod.
68	NA	IL	15	NA	Mod.
45	– (0/13)	ID	15	I	Poor
41	+ (2/14)	ID/IL	29	II	Mod.
48	– (0/6)	ID	30	I	Poor
62	– (0/14)	ID	14	I	Mod.
55	– (0/6)	ID	75	III	Mod.
58	+ (18/18)	ID	NA	III	Poor
62	+ (4/9)	ID	22	II	Mod.
63	– (0/7)	ID	28	I	Mod.
68	– (0/15)	ID	18	I	Poor
82	+ (5/7)	ID	35	III	Poor
68	+ (2/17)	ID	75	II	Mod.
31	+ (1/6)	UD	190	II	Poor
52	NA	NA	NA	NA	NA
71	+ (2/6)	ID	30	II	Mod.
68	+ (3/10)	M	30	II	Poor
80	– (0/10)	ID	15	I	Well
39	+ (5/14)	ID	15	II	Mod.

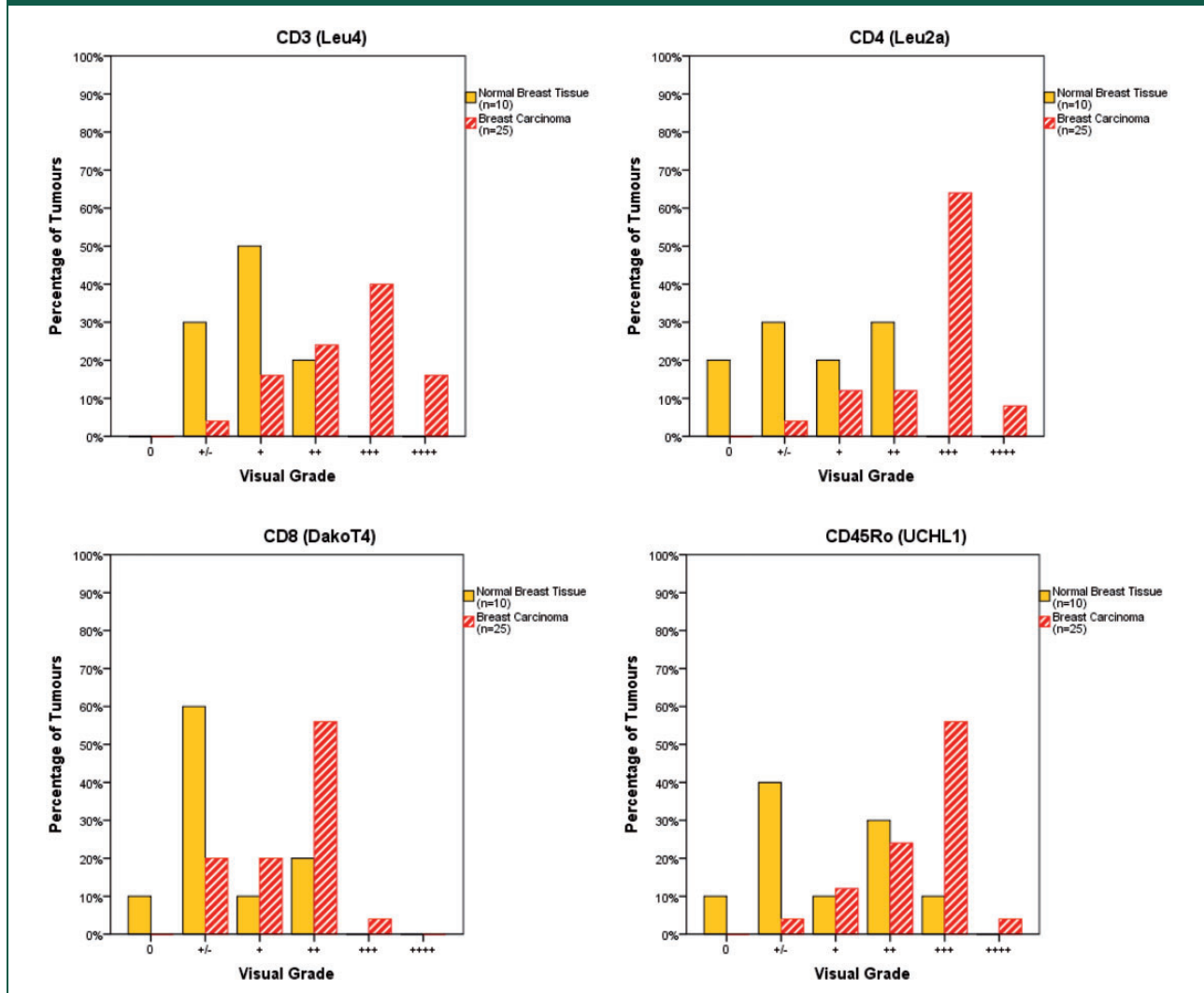
ID: infiltrating ductal; IL: infiltrating lobular; M: medullary; Mod.= moderately differentiated; NA= not available/reported; UD: undifferentiated; += tumour involved lymph node(s); – = non-tumour involved lymph node(s); (x/y)= no. of positive nodes (x) out of the total examined (y).

approximately 10% or less being  $\gamma\delta$ -TCR positive. Very small numbers of B-cells, CD16 positive cells and macrophages were located interstitially between the breast ducts. Most of the mononuclear cells in normal breast tissues were IL2 $\alpha$  receptor negative, but HLA-D and HLA-DQ positive. The duct

epithelium expressed moderate levels of HLA-D in about half the cases examined. HLA-Class I ( $\beta_2$ -microglobulin) was expressed at moderate levels on normal breast duct epithelium examined.

A novel finding was that some  $\gamma\delta$ -T cells were present in an intraepithelial location in the ducts of

**Figure 1.** Histograms comparing manual visual grades of infiltrate found in normal breast and primary breast carcinoma tissues with respect to immunostaining for various antigens.



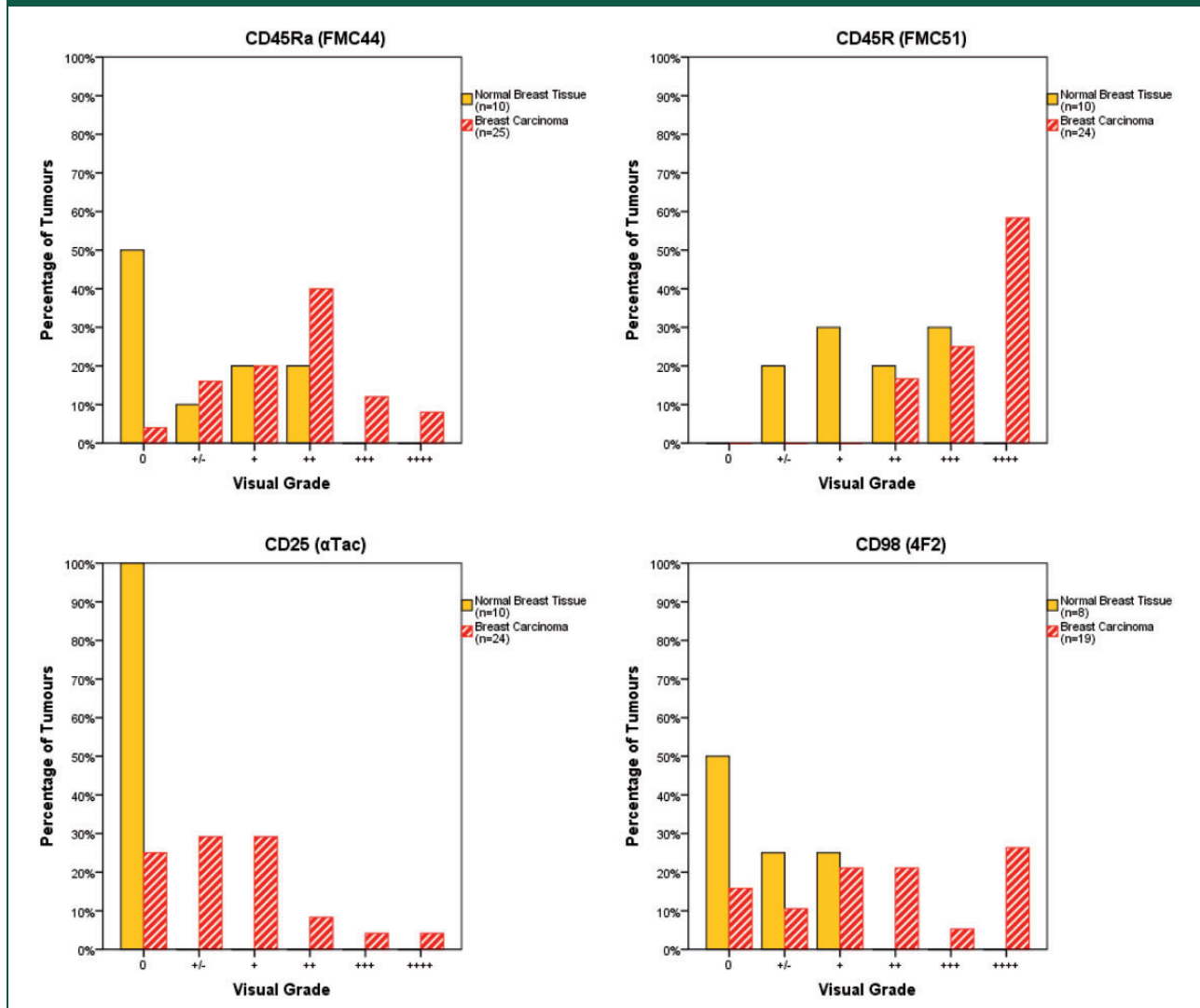
normal breast tissue (Figure 2(a)). Double immunostaining with IgA monoclonal antibodies showed these  $\gamma\delta$ -T cells to be associated with, but separate from, IgA producing cells (Figure 2(b))

**Breast carcinoma tissues.** The mononuclear infiltrate in breast carcinoma contained mainly T-cells, which were present in much larger numbers than in the normal tissues. There was a predominance of CD4 cells (T4:T8 ratio of  $>1$ ; significant) and a predominance of memory CD45RO cells over naive CD45RA cells (not statistically significant). No statistically significant difference was found between the grading of CD3 positive cells and CD4 cells in the tumour infiltrates ( $p = .978$ ), but CD4 and CD8 cell gradings were highly statistically significantly different ( $p < 0.001$ ).

The proportion of T-cells that were  $\gamma\delta$ -TCR positive was 30%, with the majority of cells constituting  $\alpha\beta$ -TCR in type. IL-2 $\alpha$  receptor expression was low or absent on TIL in all but three tumours, and HLA-D was expressed heavily on TIL in all but one tumour. HLA-DQ was expressed on almost all TIL at moderate to high levels. HLA-D was expressed on tumour cells at low levels in approximately 25% of tumours tested, whereas HLA Class I was expressed on tumour cells at moderate to high levels in 70% of tumours.

Low numbers of B-cells and CD16 positive cells were present. Macrophages were present in tumours in a greater proportion than in normal breast tissues. Notably, CD45 labelled more cells than were apparently accounted for by all cells labelled by T, B, CD16 and macrophage antibodies.

Figure 1. Continued.



When breast tumour tissues were compared with normal tissues, the excess numbers of CD3, CD4, CD45RO, CD45RA(2H4), CD45 and HLA Class II (on TIL) were statistically significant ( $p < .01$ , Kolmogorov–Smirnov). CD19 (B-cell), CD14 (FMC32 & 33) and HLA Class I levels (epithelial and TIL) showed no statistically significant differences.

### Video image analysis

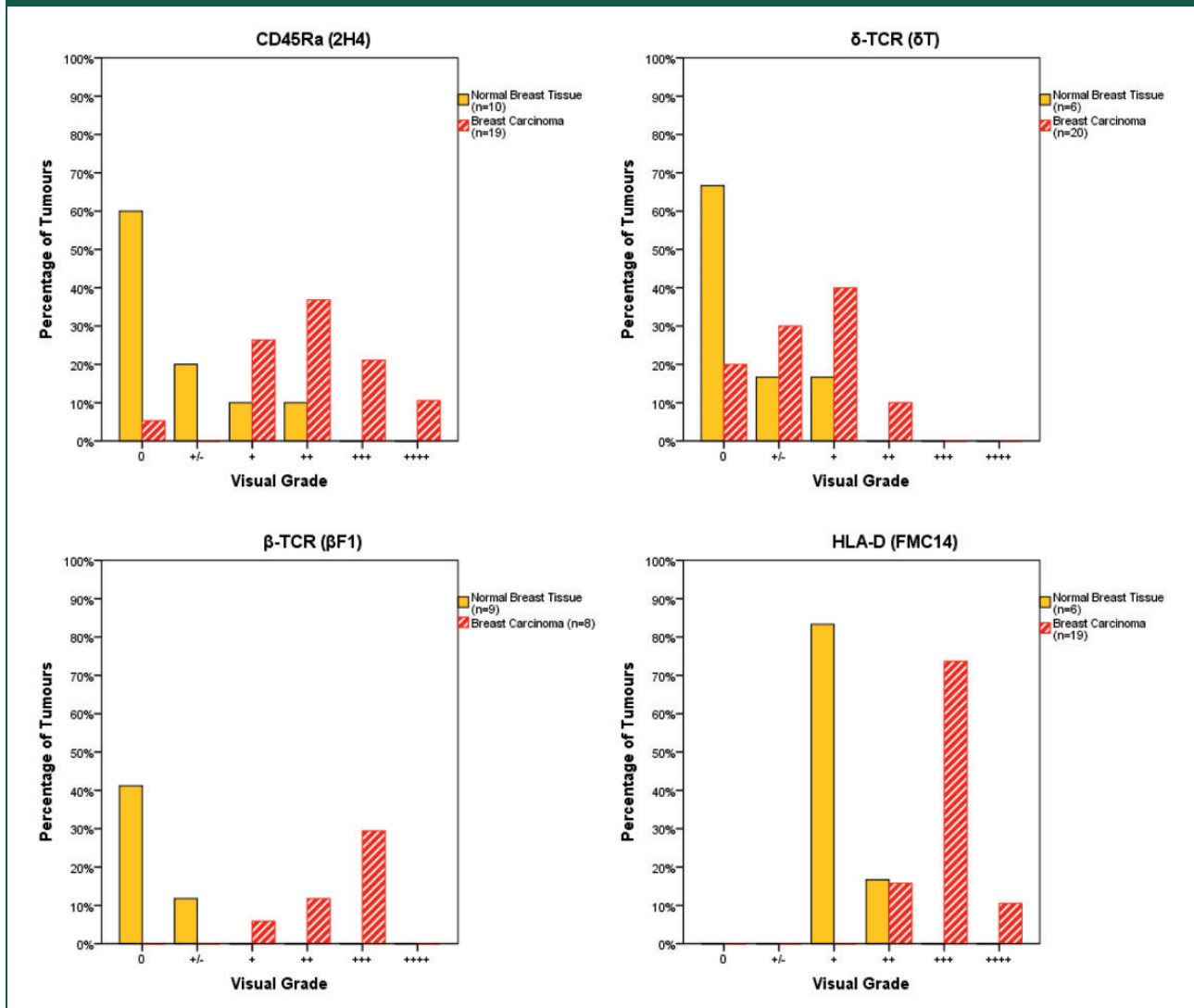
The results from VIA assessment of the same immunoperoxidase-stained tissue sections used for the direct visual quantitation data above are depicted in Figure 3. Results for the average area under each of the CD3 curves and direct visual grades for each

case have previously been published.<sup>28</sup> Data in Table 3 depict the VIA pixel measurements in ascending order of magnitude for the 20 individual breast cancer specimens stained with CD3, with the corresponding ordinal grade measured by manual visual method for each particular tumour shown alongside.

### Associations between VIA pixel values and age/tumour size

Associations between pixel values and both age (in years)/tumour size (diameter in millimetre) were assessed using Pearson correlation coefficients. Table 4 shows that VIA pixel values were significantly

Figure 1. Continued.



correlated with tumour size, whereas the correlation between VIA pixel values and age approached significance.

### Associations between VIA pixel values and lymph node status, TNM stage and differentiation as assessed using independent samples *t*-Tests

Table 5 shows no evidence for a significant difference in mean VIA pixel values between lymph node negative and lymph node positive patients ( $t_{18} = 0.060$ ,  $p = 0.56$ ). Similarly, no evidence was found for a statistical difference in mean VIA pixel values between TNM Stage I and Stage II/III patients ( $t_{18} = 0.070$ ,  $p = 0.49$ ). Last, no statistical difference was evident between mean VIA pixel values for patients with

well to moderately differentiated compared to poorly differentiated breast tumours ( $t_{18} = -0.075$ ,  $p = .46$ ).

### Discussion

Detailed immune profiles of breast carcinomas and normal breast tissues were reported in this study, which is of increased relevance given the current interest in immunotherapeutic approaches to breast cancer management.<sup>29,30</sup> The most sensitive techniques were used to obtain a detailed analysis of major subpopulations within the lymphoid infiltrate in breast carcinoma and normal breast tissues. By combining high-sensitivity, heavy metal enhanced di-aminobenzidine immunoperoxidase staining methods with computer-assisted video image analysis for cell quantitation, the most accurate evaluation was

Figure 1. Continued.

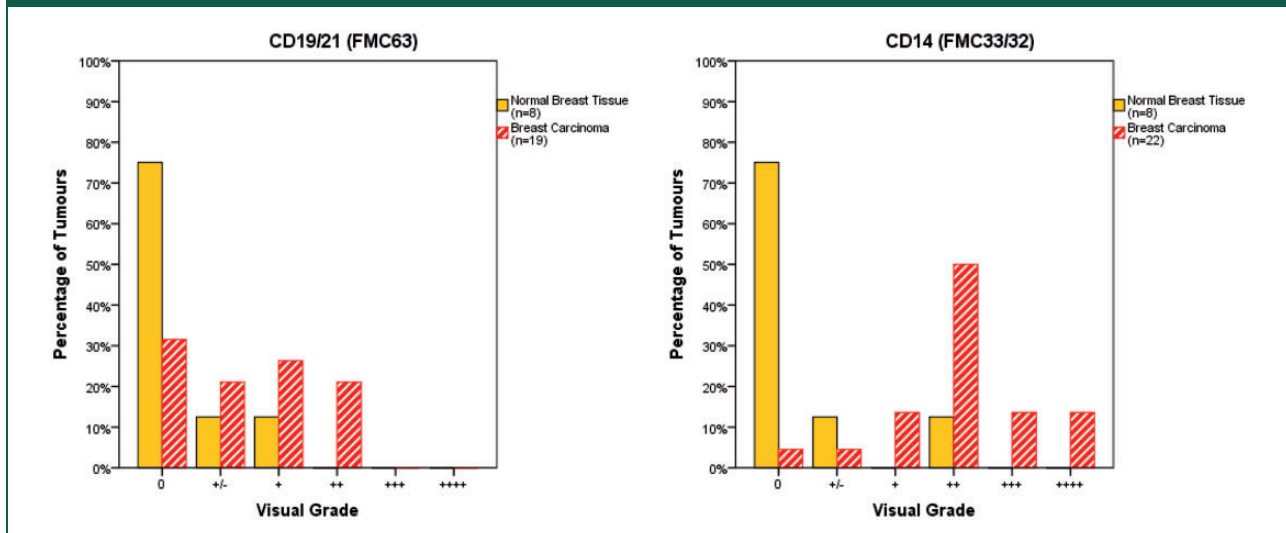
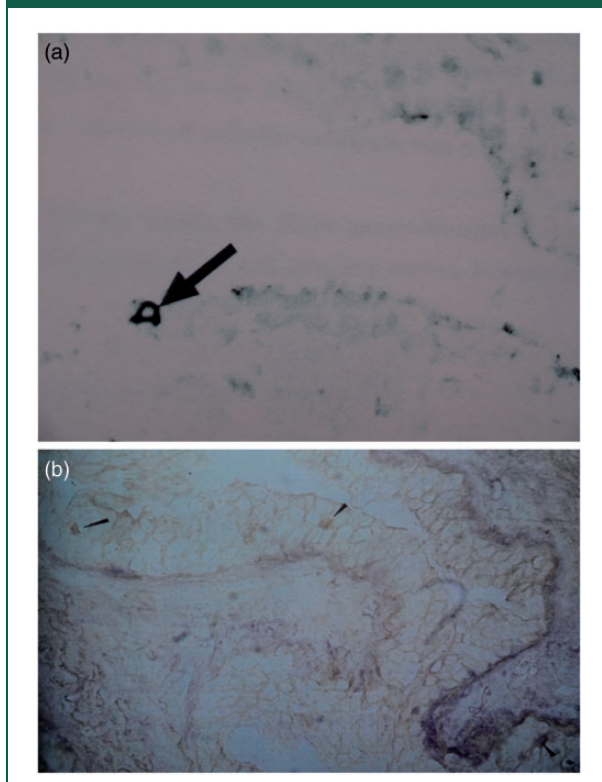


**Figure 2.** (a) High-sensitivity staining showing a  $\gamma\delta$ -T cell in an intraepithelial location between ductal cells of normal breast tissue. (b) Intraepithelial  $\gamma\delta$ -T cell shown associated with IgA-producing cells using double staining with IgA monoclonal antibodies.



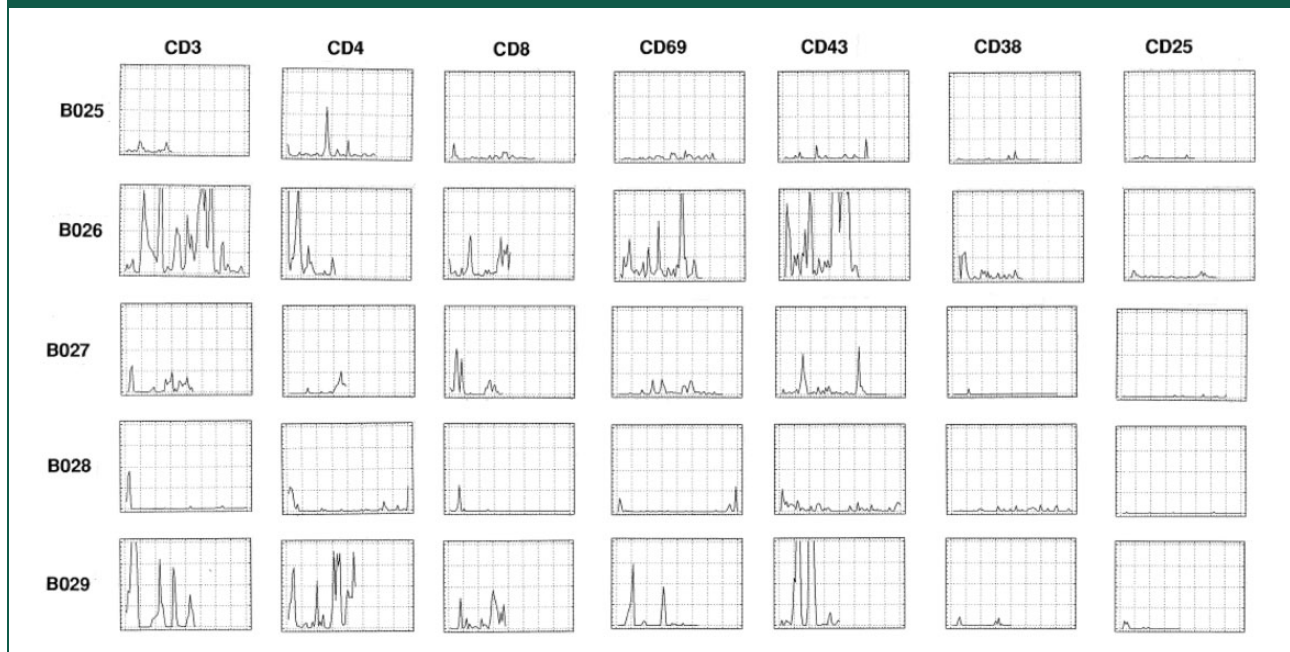
possible, and this was compared with standard manual visual quantitation.

This revealed several major qualitative and quantitative differences in the cellular infiltrates of both normal and malignant breast tissues. T-lymphocytes were present in very low numbers around breast ducts in normal tissues but were present in large numbers within and around breast carcinomas. Some 90% of tumours were shown to have infiltrates of ++ or greater compared to 20% for normal breast tissues. Most of the T-cells were CD45RO indicating previous antigen priming<sup>31</sup> and the proportion of CD4 cells was greater in tumours. The proportion of  $\gamma\delta$ -TCR positive cells was also greater in tumour tissues, perhaps suggesting less specific T-cell mechanisms might also be operational in the tumour microenvironment. An observation which might also support this notion were the increased macrophage numbers associated with tumour tissue compared to normal tissues, with over 75% of tumour samples having a ++ or greater infiltrate compared to 12% for normal tissues. B-lymphocytes were slightly increased in tumour tissues over normal tissues, but the B-cell infiltrate was sparse even in tumours. Similarly, sparse infiltration of CD57 positive cells (neutrophils) was noted in both tumours and normal tissues.

Collectively, these results show that tumour tissues possess a clearly different leukocyte infiltrate to normal breast tissues. Quantitative differences were present in T-cell and macrophage numbers; in addition, qualitative differences were found. CD4 to CD8



**Figure 3.** Video image analysis graphical profiles for serial sections from five separate tumours immunoperoxidase stained using various primary antibodies for comparison with direct visual quantitation data in Figure 1. Vertical axis is density of staining; Horizontal axis is distance across the tissue section.<sup>28</sup> Axes are the same for all graphs shown.



subgroup proportions,  $\delta$ -TCR positive cells and CD45RO positive cells were all elevated in tumours. These findings suggest that T-cells, and to a lesser extent macrophages, either proliferate or are attracted to the tumour microenvironment to aggregate in considerable numbers in most of the breast tumours examined. Most of these cells display the 180,000 kDa form of the leukocyte common antigen implying previous antigen priming and cellular activation.<sup>32</sup> Expression of the CD25 molecule as a marker of early activation was very low in normal breast tissue and also low in the infiltrating cell population associated with breast tumours, supporting other studies.<sup>33,34</sup> CD4 cells appeared to predominate over CD8 cells in the breast tumours tested.

T-cells consisting of mainly  $\alpha\beta$ -TCR CD4 cells comprise the major component of the tumour infiltrate of breast tumours, and possess the CD45RO phenotype, are HLA class II positive in 95% of tumours examined and show almost uniform absence or very low expression of the p55 and p70 chains of the IL-2R. Taken together, these findings suggest that the lymphocytes have been exposed to antigen, but are not activated, being down-regulated. Considering the data from VIA quantitation of immunostained cells from the same tumour sections as used for direct visual assessment, several features are apparent. Clustering of CD3 cells within the tumour is notable from the profiles, and considerable variations are

observed between the direct visual grade and the area under the VIA curve. The limitations imposed by the quantal nature of the direct visual grading method become apparent from this comparison.

Novel VIA techniques appeared to be a useful tool that allows for quantitatively correlating staining density as a continuous variable with various patient characteristics. Such analysis has often been difficult previously. Staining density was shown to correlate positively with tumour size, but no association was found with lymph node status, TNM stage or degree of differentiation. This is likely due to the small sample size, although one of the potential benefits of VIA is that larger studies can be conducted more easily, compared with time-intensive and slower manual visual grading.

The VIA methods in this study also provided graphical profiles for each of the different antibodies. This allowed more detailed representation of the pattern of distribution of the subpopulations of lymphoid infiltrate within the tumour. Features such as clustering of cell types can also be observed and quantitated using VIA.<sup>28</sup> Moreover, it also allowed for the association comparison of areas within the tumour where cellular subgroups could be identified as either overlapping or distinct. Analysis of cytokine expression and cytokine receptor expression within the tumour microenvironment using these methods is under current investigation.

**Table 3.** Comparison of VIA pixel value with assigned manual visual grade.

VIA pixel value	Manual visual grade
488	+++
962	+/-
1070	++
1786	+
3726	+++
3856	++
4193	++
7353	++
9013	++
9899	++++
10,260	+
12,949	+++
16,400	+++
16,597	+++
28,036	+++
32,901	++
34,352	++++
36,349	+++
40,108	+++
42,753	++++

Our previous work demonstrated that both dendritic cell number and activation were low in human breast cancers and showed an association between density of CD1a cells and five-year survival, although non-significant at the  $p = .05$  level.<sup>35,36</sup>

The importance of the current findings and techniques used in this study are that better understanding of the distribution of the tumour infiltrating leukocyte population within human breast carcinomas is now possible. Further work is revealing the implications of TIL characteristics for clinical outcome, including longer term survival, which is currently being actively evaluated in greater detail.

**Table 4.** VIA pixel density correlated with patient age and tumour size.

	Age	Tumour size
VIA pixel density	$r = -0.42$	$r = 0.45$
	$p = 0.067$	$p = 0.048$

Pearson correlation coefficients;  $n = 20$ .

**Table 5.** VIA pixel density correlated with lymph node status, TNM stage and tumour differentiation.

VIA pixel density and lymph node status			
Lymph node status	Number	Mean	Standard deviation
Negative	8	18,065.00	$\pm 13,540.5$
Positive	12	14,044.30	$\pm 15,514.5$
VIA pixel density and TNM stage			
TNM stage	Number	Mean	Standard deviation
I	7	18,795.90	$\pm 14,454.0$
II/III	13	13,960.00	$\pm 14,857.1$
VIA pixel density and tumour differentiation			
Differentiation	Number	Mean	Standard deviation
Moderate/well	11	13,416.90	$\pm 13,596.5$
Poor	9	18,385.00	$\pm 15,960.5$

## Conclusion

The results obtained in this study indicate that although primed T-cells predominate, other immunological cell types are present. These other cell types and the relationship to the structural morphology and interaction with CD3 cells require further investigation. Indeed, significant interaction or cooperation between cell types in the tumour inflammatory infiltrate likely does occur. More detailed analysis of the distribution of immunological cells within the TIL infiltrate using high-sensitivity immunostaining and VIA techniques offers a logical approach recommended for further investigations in this area. The potential importance and significance of these findings lie in the association between breast cancer TIL immune profile and clinical outcome, including survival.

## Declarations

**Competing Interests:** None declared

**Funding:** Funding was received from the Royal Australasian College of Surgeons and the National Health and Medical Research Council of Australia, in the form of Research Fellowships. Financial support for this study was provided from the National Health and Medical Research Council of Australia (Research Fellowship), Anti-cancer Foundation of the Universities of South Australia, and the Royal Australasian College of Surgeons Research Foundation. Antibodies were generously provided by Dr Michael Brenner, Boston, USA ( $\gamma\delta$ -TCR), Professor Peter Beverley, University College London, UK (UCHL-1) and Professor Heddy Zola, Flinders Medical Centre, Adelaide, Australia (FMC14, FMC32, FMC33, FMC44, FMC51, FMC63).

**Ethical approval:** Flinders Medical Centre Human Ethics Committee.

**Guarantor:** BJC

**Contributorship:** BJC performed the immunohistochemical studies; BJS, JMS and JB examined the slides to provide scores; BJC did the image analysis; BJS and MJW performed the statistical analysis; BJC & MJW wrote the manuscript and all authors read and contributed to it.

**Acknowledgements:** The authors would like to thank Peter Graff, Paul Stoll and Lynn Jarvis for their encouragement and assistance in the image analysis work and Mohd Norazmi for initial help with the immunohistochemistry. The authors also thank the surgeons, Drs Neil MacIntosh, Clive Hoffman, Elizabeth Cant, Richard Hamilton, Gwyn Morgan and John Hokin for their generous support and help with specimen collection.

**Provenance:** Not commissioned; peer-reviewed by Angus Dalgleish

**Reviewer:** Angus Dalgleish

## References

- Zhang L, Conejo-Garcia JR, Katsaros D, Gimotty PA, Massobrio M, Regnani G, et al. Intratumoral T cells, recurrence, and survival in epithelial ovarian cancer. *N Engl J Med* 2003; 348: 203–213.
- Hussein MR and Hassan HI. Analysis of the mononuclear inflammatory cell infiltrate in the normal breast, benign proliferative breast disease, in situ and infiltrating ductal breast carcinomas: preliminary observations. *J Clin Pathol* 2006; 59: 972–977.
- Hussein MR, Elsans DAH, Fadel SA and Omar A-EM. Immunohistological characterisation of tumour infiltrating lymphocytes in melanocytic skin lesions. *J Clin Pathol* 2006; 59: 316–324.
- Loughlin PM, Cooke TG, George WD, Gray AJ, Stott DI and Going JJ. Quantifying tumour-infiltrating lymphocyte subsets: a practical immuno-histochemical method. *J Immunol Methods* 2007; 321: 32–40.
- Pagès F, Berger A, Camus M, Sanchez-Cabo F, Costes A, Molidor R, et al. Effector memory T cells, early metastasis, and survival in colorectal cancer. *N Engl J Med* 2005; 353: 2654–2666.
- Lee AH, Gillett CE, Ryder K, Fentiman IS, Miles DW and Millis RR. Different patterns of inflammation and prognosis in invasive carcinoma of the breast. *Histopathology* 2006; 48: 692–701.
- Schmidt M, Böhm D, von Töme C, Steiner E, Puhl A, Pilch H, et al. The humoral immune system has a key prognostic impact in node-negative breast cancer. *Cancer Res* 2008; 68: 5405–5413.
- DeNardo DG, Brennan DJ, Rexhepaj E, Ruffell B, Shiao SL, Madden SF, et al. Leukocyte complexity in breast cancer predicts overall survival and functionally regulates response to chemotherapy. *Cancer Discov* 2011; 1: 54–67.
- Loi S, Sirtaine N, Piette F, Salgado R, Viale G, van Eenoo F, et al. Prognostic and predictive value of tumor-infiltrating lymphocytes in a phase III randomized adjuvant breast cancer trial in node-positive breast cancer comparing the addition of docetaxel to doxorubicin with doxorubicin-based chemotherapy: BIG 02-98. *J Clin Oncol* 2013; 31: 860–867.
- Denkert C, Loibl S, Noske A, Roller M, Müller BM, Komor M, et al. Tumor-associated lymphocytes as an independent predictor of response to neoadjuvant chemotherapy in breast cancer. *J Clin Oncol* 2010; 28: 105–113.
- West NR, Milne K, Truong PT, Macpherson N, Nelson BH and Watson PH. Tumor-infiltrating lymphocytes predict response to anthracycline-based chemotherapy in estrogen receptor-negative breast cancer. *Breast Cancer Res* 2011; 13: R126.
- Ono M, Tsuda H, Shimizu C, Yamamoto S, Shibata T, Yamamoto H, et al. Tumor-infiltrating lymphocytes are correlated with response to neoadjuvant chemotherapy in triple-negative breast cancer. *Breast Cancer Res Treat* 2012; 132: 793–805.
- Dieci MV, Criscitiello C, Goubar A, Viale G, Conte P, Guarneri V, et al. Prognostic value of tumor-infiltrating lymphocytes on residual disease after primary chemotherapy for triple-negative breast cancer: a retrospective multicenter study. *Ann Oncol* 2014; 25: 611–618.
- Schalper KA, Velcheti V, Carvajal D, Wimberly H, Brown J, Pusztai L, et al. In situ tumor PD-L1 mRNA expression is associated with increased TILs and better outcome in breast carcinomas. *Clin Cancer Res* 2014; 20: 2773–2782.
- Yu P and Fu YX. Tumor-infiltrating T lymphocytes: friends or foes? *Lab Invest* 2006; 86: 231–245.
- Gisterek I, Frydecka I, Światonowski G, Fidler S and Kornafel J. Tumour-infiltrating CD4 and CD8 T lymphocytes in breast cancer. *Rep Pract Oncol Radiother* 2008; 13: 206–209.
- Mahmoud SM, Paish EC, Powe DG, Macmillan RD, Grainge MJ, Lee AH, et al. Tumor-infiltrating CD8+ lymphocytes predict clinical outcome in breast cancer. *J Clin Oncol* 2011; 29: 1949–1955.
- Daniel D, Meyer-Morse N, Bergsland EK, Dehne K, Coussens LM and Hanahan D. Immune enhancement of skin carcinogenesis by CD4+ T cells. *J Exp Med* 2003; 197: 1017–1028.
- Gianni L, Zambetti M, Clark K, Baker J, Cronin M, Wu J, et al. Gene expression profiles in paraffin-embedded core biopsy tissue predict response to

- chemotherapy in women with locally advanced breast cancer. *J Clin Oncol* 2005; 23: 7265–7277.
20. Hornychova H, Melichar B, Tomsova M, Mergancova J, Urminska H and Ryska A. Tumor-infiltrating lymphocytes predict response to neoadjuvant chemotherapy in patients with breast carcinoma. *Cancer Invest* 2008; 26: 1024–1031.
  21. Robins RA. T-cell responses at the host: tumour interface. *Biochim Biophys Acta* 1986; 865: 289–305.
  22. Coventry BJ, Neoh SH, Mantzioris BX, Skinner JM, Zola H and Bradley J. A comparison of the sensitivity of immunoperoxidase staining methods with high-sensitivity fluorescence flow cytometry-antibody quantitation on the cell surface. *J Histochem Cytochem* 1994; 42: 1143–1149.
  23. Coventry BJ, Bradley J and Skinner JM. Differences between standard and high-sensitivity immunoperoxidase staining methods in tissue sections – comparison of immunoperoxidase staining methods using computerised video image analysis. *Pathology* 1995; 27: 221–223.
  24. Kraan MC, Haringman JJ, Ahern MJ, Breedveld FC, Smith MD and Tak PP. Quantification of the cell infiltrate in synovial tissue by digital image analysis. *Rheumatology (Oxford)* 2000; 39: 43–49.
  25. Walker RA. Quantification of immunohistochemistry – issues concerning methods, utility and semiquantitative assessment I. *Histopathology* 2006; 49: 406–410.
  26. Bernardo V, Lourenço SQ, Cruz R, Monteiro-Leal LH, Silva LE, Camisasca DR, et al. Reproducibility of immunostaining quantification and description of a new digital image processing procedure for quantitative evaluation of immunohistochemistry in pathology. *Microsc and Microanal* 2009; 15: 353–365.
  27. Benali A, Leefken I, Eysel UT and Weiler E. A computerized image analysis system for quantitative analysis of cells in histological brain sections. *J Neurosci Methods* 2003; 125: 33–43.
  28. Coventry BJ, Weightman MJ, Skinner JM and Bradley J. Improving evaluation of the distribution and density of immunostained cells in breast cancer using computerized video image analysis. *Cancer Manag Res* 2011; 3: 101–108.
  29. Milani A, Sangiolo D, Aglietta M and Valabrega G. Recent advances in the development of breast cancer vaccines. *Breast Cancer: Targets and Therapy* 2014; 6: 159–168.
  30. Criscitiello C, Esposito A, Gelao L, Fumagalli L, Locatelli M, Minchella I, et al. Immune approaches to the treatment of breast cancer, around the corner? *Breast Cancer Res* 2014; 16: 204–202.
  31. Merckenschlager M and Beverley PCL. Evidence for differential expression of CD45 isoforms by precursors for memory-dependent and independent cytotoxic responses: human CD8 memory CTLp selectively express CD45RO (UCHL1). *Int Immunol* 1989; 1: 450–459.
  32. Wallace DL and Beverley PCL. Phenotypic changes associated with activation of CD45RA<sup>+</sup> and CD45RO<sup>+</sup> T-cells. *Immunology* 1990; 64: 460–467.
  33. Whiteside TL, Mieschner S, Hurlimann J, Moretta L and von Flidner V. Clonal analysis and in-situ characterization of lymphocytes infiltrating human breast carcinomas. *Cancer Immunol Immunother* 1986; 23: 169–178.
  34. Whiteside TL, Miescher S, Hurlimann J, Moretta L and von Flidner V. Separation, phenotyping and limiting dilution analysis of T-lymphocytes infiltrating human solid tumours. *Int J Cancer* 1986; 37: 803–811.
  35. Coventry BJ, Lee PL, Gibbs D and Hart DN. Dendritic cell density and activation status in human breast cancer – CD1a, CMRF-44, CMRF-56 and CD-83 expression. *BJC* 2002; 86: 546–551.
  36. Coventry BJ and Morton J. CD1a-positive infiltrating dendritic cell density and five year survival from human breast cancer. *BJC* 2003; 89: 533–538.